RESEARCH ARTICLE | APRIL 28 2023

Structural and chemical bonding properties of blood shells–based hydroxyapatite: Effect of temperature sintering

Nurlaela Rauf ✉; Fitria Hamza Lahu; Sri Suryani

AIP Conference Proceedings 2619, 050011 (2023)
https://doi.org/10.1063/5.0122602

Structural and Chemical Bonding Properties of Blood Shells–Based Hydroxyapatite: Effect of Temperature Sintering

Nurlaela Rauf[1,a)], Fitria Hamza Lahu[1,b)], Sri Suryani[1,c)]

[1]*Department of Physics, Faculty of Mathematics and Natural Sciences, University of Hasanuddin, Makassar 90245, Indonesia*

[a)] Corresponding author: n-rauf@fmipa.unhas.ac.id
[b)]fitrihamza13@gmail.com
[c)]sri_sumah@yahoo.com

Abstract. Synthesis of hydroxyapatite shells of blood clams (*Anadara granosa*) has been carried out using the precipitation method. This research was conducted to determine the effect of variations in sintering temperature on the synthesis of hydroxyapatite blood clam shells, namely 700, 800, 900, and 1000℃ for 5 hours. Characterization was carried out using XRF, FTIR, XRD and testing the mass efficiency of hydroxyapatite. The XRF analysis showed that the blood clam shells was 99.92% $CaCO_3$ before calcination and 99.49% CaO after calcination. The hydroxyapatite contains chemical compounds, namely CaO and P_2O_5, with a CaO/P_2O_5 ratio of 1.51 - 1.77. The functional groups of phosphate (PO_4^{3-}), hydroxyl (OH^-), and carbonate (CO_3^{2-}) were observed in the FTIR of hydroxyapatite. These functional groups indicate that hydroxyapatite has been formed at each temperature variation. The XRD analysis showed that hydroxyapatite has a hexagonal crystal structure. This result is the same as the crystal structure of commercial hydroxyapatite. The purity of the hydroxyapatite produced is not optimum because there is still a secondary phase of HAp decomposition. At a temperature of 1000℃, the average value of the hydroxyapatite crystal size is 15.40 nm. Hydroxyapatite efficiency value decreased with increasing sintering temperature.

INTRODUCTION

The development of research is growing along with the increasing development of technology, one of which is the development of research in the field of materials which has been proven to provide enormous benefits in human life. The utilization of natural materials and wasted waste makes research in materials develop rapidly due to the availability of abundant materials at low costs. One of the fields of material that is widely used as the object of research at this time is bio-ceramics. Bio-ceramics are widely developed because they have many advantages, including resistance to high temperatures and easy-to-obtain materials. They have several uses widely applied in the health sector, one of which is an implant or replacement organ [1,2].

One of the synthetic materials being developed is hydroxyapatite bio-ceramic. Hydroxyapatite (HAp) is a calcium phosphate compound that has the molecular formula $Ca_{10}(PO_4)_6(OH)_2$ [3,4]. HAp is widely used in biomedical applications, especially as bone substitutes and dental restorative materials, because of its good biocompatibility, non-toxicity, environmental friendliness, good bioactivity, and osteoconductivity [5,6]. In addition, the structure of HAp is chemically similar to the mineral phase of human bone and teeth [2,7]. The synthesis of hydroxyapatite can be carried out by several methods, namely the precipitation method, hydrothermal method, double emulsion technique, and the sol-gel method [8-11]. The synthesis method that can be used in this research is the precipitation method. This method is widely used because the process is simple, low cost, relatively simple chemical reactions, and the homogeneity of the particle size obtained tends to be quite good [5, 12-13].

The 1st International Conference on Science Education and Sciences
AIP Conf. Proc. 2619, 050011-1–050011-7; https://doi.org/10.1063/5.0122602
Published by AIP Publishing. 978-0-7354-4446-1/$30.00

Hydroxyapatite can be synthesized from natural materials, namely egg shells, clam shells, coral, and animal bones [14]. As a maritime country, one of the natural ingredients that can be developed into hydroxyapatite in Indonesia is blood clam shell waste (*Anadara granosa*) [15]. Blood clam shell waste (*Anadara granosa*) is rich in calcium carbonate ($CaCO_3$), which is about 98% and potential for hydroxyapatite (HAp) source of calcium [3].

The sintering process is a process that affects the synthesis of hydroxyapatite [16]. The sintering process is heating (burning the material) without exceeding its melting point [14]. Based on previous research, HAp that undergoes a sintering process forms a very coherent bond with bone tissue [17]. The grain size, porosity, calcium/phosphorus (Ca/P) ratio, and mechanical properties of bio-ceramics are affected by the sintering temperature [6]. The sintering temperature for HAp can reach 1250^{o}C [18].

MATERIALS AND METHODS

The materials used in this study were: Blood clam shells (Anadara Granosa), diammonium hydrogen phosphate ($(NH_4)_2HPO_4$), and distilled water.

The blood clam shells were cleaned using clean water to remove organic matter, and dirt adhering to the shells, then dried for 6 hours. The cleaned shells were crushed using a hammer into small flakes, then crushed again by grinding using a mortar to form smaller particles in a blender to form fine powder particles. The blood clam shell powder was then sieved using a 200 mesh sieve. Then it was calcined at 900℃ for 5 hours to get CaO powder.

About 2.83 grams of CaO powder and 3.97 grams $(NH_4)_2HPO_4$ mixing by precipitation method. The CaO powder was dissolved in 100 mL of distilled water then stirred at a speed of 350 rpm using a magnetic stirrer for 10 minutes, marked as the first solution. ($(NH_4)_2HPO_4$ was dissolved with 100 mL distilled water and stirred at 350 rpm using a magnetic stirrer for 10 minutes, marked as the second solution. The deposition method is carried out by the titration method. The second solution drops into the first solution at a flow rate of 10 ml/minute and is stirred with a magnetic stirrer using a speed of 350 rpm until the solution homogeny. The homogeny solution of $(NH_4)_2HPO_4$ is then covered with aluminum foil and kept for 18 hours. The precipitate solution was filtered using Whitman paper, washed with distilled water, and then heated at 110℃ for 3 hours. The sintering process was carried out at 700, 800, 900, and 1000℃ for 5 hours.

Hydroxyapatite mass efficiency was calculated using the formula [19]:

$$\text{Hydroxyapatite mass efficiency (\%)} = \frac{\text{hydroxyapatite mass after sintering}}{\text{initial mass of calcium and phosphoric acid}} \text{ x } 100\% \quad (1)$$

The chemical composition of blood clam shell (*Anadara Granosa*) was carried out using X-ray fluorescence (XRF) for before and after calcination, and the functional groups of HAp were analyzed using Fourier Transform Infrared (FTIR). The structural properties, including crystallite size and lattice parameters, were analyzed from the X-Ray Diffraction (XRD) spectra. The crystallite size calculated using the Scherer's equation as follows [20]:

$$D = \frac{0{,}9\,\lambda}{\beta \cos\theta} \quad (2)$$

RESULTS AND DISCUSSION

X-Ray Fluorescence (XRF) Analysis

Blood clam shells were used as raw material in the preparation of hydroxyapatite. Based on research that Awang-Hazmi has carried out at el. blood clam shells used as raw materials for the synthesis of hydroxyapatite have a high calcium content in the form of calcium carbonate ($CaCO_3$), which is 98.7% [21]. XRF analysis results show that the largest content of the blood clam shells is 99.92% of $CaCO_3$ and 0.08% of other chemical compositions. The high calcium content in blood clam shells makes this material very potential to be used as raw material for the synthesis of hydroxyapatite.

Calcination of clam shell powder at a temperature of 900ºC for 5 hours using a furnace aims to convert $CaCO_3$ compounds into CaO, with the reaction equation [22]:

$$CaCO_3 \rightarrow CaO + CO_2 \uparrow \quad (3)$$

Calcination can also remove organic compounds and impurities that interfere with the formation of HAp [16, 23]. The results obtained are white powder with a calcium oxide (CaO) content of 99.49% and other chemical compositions of 0.51%. The presence of oxide compounds other than CaO is caused by other compounds that react when the synthesis process is carried out [24].

The hydroxyapatite based on blood clam shells (*Anadara granosa*) using the precipitation method for various sintering temperatures has been successfully carried out. The reaction equation for the formation of the compound HAp is illustrated by a chemical in the following equation [4]:

$$10Ca(OH)_2 + 6(NH_4)_2HPO_{4(s)} + 2H_2O_{(aq)} \rightarrow Ca_{10}(PO_4)_6(OH)_{2(s)} + 12\ NH_4OH_{(aq)} + 6H_2O_{(aq)} \quad (4)$$

TABLE 1. Results of XRF analysis of HAp powder (RT is room temperature).

Temperature	Oxide compounds				Ratio
	CaO	P_2O_5	SrO	Other	CaO/P_2O_5
RT	60.08	39.72	0.10	0.09	1.51
700 °C	60.58	39.23	0.18	0.01	1.54
800 °C	62.94	36.87	0.18	0.01	1.70
900 °C	63.70	36.02	0.21	0.07	1.77
1000 °C	63.58	36.03	0.24	0.15	1.76

The resulting hydroxyapatite composition contains the main chemical compounds, namely CaO and P_2O_5, with the ratio of 1.70 from hydroxyapatite with a sintering temperature of 800 C, which is closest to the stoichiometric CaO/P_2O_5 ratio of hydroxyapatite, which is 1.67 [25]. The key factor that causes deviations in the CaO/P_2O_5 ratio of stoichiometry is the sintering temperature which is typical for bioceramics [26].

Fourier Transform Infrared (FTIR) Analysis

The FTIR spectra of samples with varying sintering temperatures of 700, 800, 900, and 1000°C are presented in Figure 1. Hydroxyapatite contains OH^- group, CO_3^{2-} group, and PO_4^{3-} group [27].

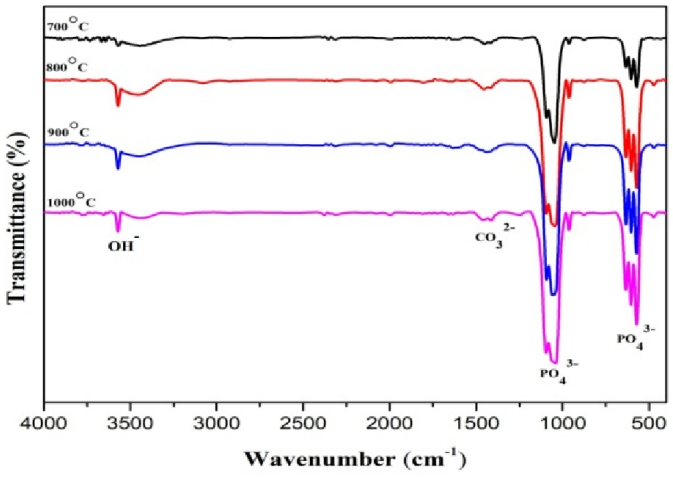

FIGURE 1. FTIR spectrum of hydroxyapatite of blood clam shells at various sintering temperatures.

TABLE 2. Wave Number Result from the FTIR Spectrum

Wave Number (cm-1)				Functional groups
700°C	800°C	900°C	1000°C	
565, 580, 608	565, 580, 608	565, 580, 608	565, 580, 608	PO_4^{3-} asymmetry bending
1045, 1091	1045, 1091	1045, 1091	1045, 1091	PO_4^{3-} asymmetry stretching
3564	3564	3564	3564	OH^-
1450	1450	1450	1450	CO_3^{2-}

The spectrum for samples with various variations in sintering temperature showed the presence of an OH^- group absorption band at a wavenumber of 3564 cm^{-1}. Venkatesan and Kim reported that the peak at wavenumber 3300-3600 cm^{-1} corresponded to the hydroxyl group [28]. The absorption band of the phosphate group (PO_4^{3-}) has stretching asymmetric vibrations, visible at wavenumbers from 1045 cm^{-1} to 1091 cm^{-1}. The bending vibration band of PO_4^{3-} group at the wavenumbers 565 cm^{-1}, 580 $cm^{-1,}$ and 608 cm^{-1}. Mondal et al. reported the hydroxyapatite compounds at the wavenumbers of 1000-1100 cm^{-1}, stretching asymmetric and bending asymmetric vibrations of PO_4^{3-} at wavenumbers 576.30 cm^{-1} [29]. Walendra (2012) stated PO_4^{3-} and OH^- groups that appear with sharper peaks indicate a higher absorption intensity. The higher the absorption intensity, the more PO_4^{3-} and OH^- content so that the crystallinity level is getting better, which means that the hydroxyapatite obtained is getting better. The detection of the OH^- and PO_4^{3-} groups became the initial benchmark that hydroxyapatite in this study was formed at every temperature variation [30].

The synthesized carbonate (CO_3^{2-}) absorption band was detected at a wavenumber of 1450 cm^{-1}. Venkatesan and Kim stated that the absorption bands detected at wavenumbers 1414 cm^{-1} and 1457 cm^{-1} were carbonate groups [28]. The presence of carbonate ion cannot be avoided as long the HAp synthesis process is carried out in the room with open-air [31]. In general, the carbonate groups found in synthetic hydroxyapatite will replace hydroxyl or phosphate ions. This will result in a HAp of a different type than desired. The carbonate that replaces the OH^- group will produce type A hydroxyapatite carbonate. Besides that, it can form type B hydroxyapatite carbonate when the carbonate replaces the PO_4^{3-} group [32].

X-Ray Diffraction (XRD) Analysis

XRD analysis was performed to determine the crystallinity of the sample. The XRD spectrum of the hydroxyapatite compound without sintering and the different sintering temperature variations of 700, 800, 900, and 1000℃ are shown in Figure 2. Based on the XRD curve of the sample without sintering, the HAp phase formed is $2\theta = 44.332^o$ with a value of hkl (400) adapted to Joint Committee on Power Diffraction Standards (JCPDS) no. 01-072-1243. In addition to HAp in the hydroxyapatite sample without sintering, there was another phase, namely A-type carbonate apatite (AKA). The results in this study are similar to the study reported by Balgies et al. (2011) for the emergence of AKA at the low temperature of 110℃ [33].

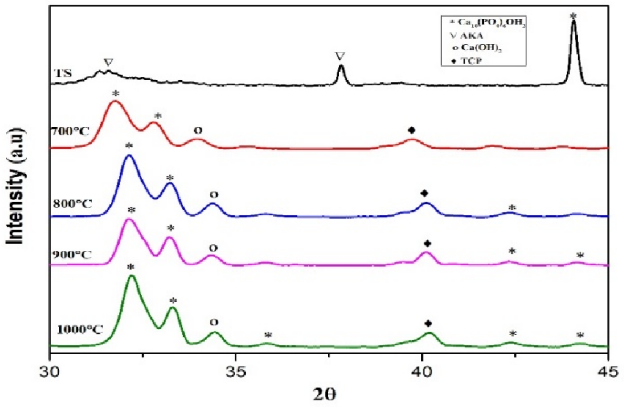

Figure 2. Hydroxyapatite XRD curve without sintering and sintering temperature variations 700, 800, 900, and 1000℃.

The results of the analysis of hydroxyapatite samples with a sintering temperature of 1000℃ contained the hydroxyapatite phase at the peak of 2θ = 32.195°; 32.897°; 34.063°; 42.325° and 43.876° which correspond to JCPDS card no: 01-074-0566 with hkl values (112), (300), (202), (302) and (113) respectively. The results of the diffractogram of HAp synthesis using the precipitation method showed that the dominant phase formed was hydroxyapatite, which was seen at the peaks of high and low-intensity angles. The crystal structure of HAp is hexagonal with lattice parameters is a = b = 9.4240 and c = 6.8790, which is similar to the crystal structure of commercial HAp [34]. The purity of the resulting HAp is not yet optimum because there is still a secondary phase of HAp decomposition. The secondary phase consists of other compounds such as $Ca(OH)_2$ and tri-calcium phosphate (TCP) [35,36]. Other research conducted by Kamalanathan et al. found the emergence of a secondary phase due to insufficient use of calcium or phosphorus precursors [37]. At temperature 1000ºC, $Ca(OH)_2$ was detected at 2θ=33.990° (JCPDS card no: 01-076-0570). Meanwhile, tricalcium phosphate for a temperature of 1000ºC was detected at an angle of 2θ=40.227° (JCPDS card no: 01-070-0364).

Tricalcium phosphate (TCP) is a calcium phosphate compound that can be used as a bone substitute with the chemical formula $Ca_3(PO_4)_2$ [38]. The phase composition of HAp/TCP occurs due to the decomposition of several HAp into the same TCP phase as reported in other studies. Partial decomposition of HAp is associated with changes in the value of the Ca:P ratio due to deficiency of calcium, phosphate, or both elements in the sample at high temperatures [39]. After comparison, it can be concluded that the synthesized HAp diffractogram has almost the same value and is similar to the standard HAp diffractogram [40].

Table 3. Effect of sintering temperature on HAp crystal size

Temperature (ºC)	FWHM (deg)	Crystal Size (nm)
700ºC	0.012613	11.71
800ºC	0.010415	14.22
900ºC	0.011717	12.36
1000ºC	0.009841	15.40

The average value of crystal size shows the relationship with the XRD curve of Hydroxyapatite with sintering temperatures of 700, 800, 900, and 1000℃. The higher peak intensity of XRD spectra, the higher crystallite size HAp for the small value of FWHM and vice versa [41], and similar reported by Balgies et al. [33].

Mass Efficiency of Hydroxyapatite

The mass efficiency of hydroxyapatite compounds from CaO and compounds $(NH_4)_2HPO_4$ can be calculated using equation 1. We can see that the mass of hydroxyapatite compounds after sintering is much smaller than the total mass of CaO and $(NH_4)_2HPO_4$ compounds which is 6.8 grams. It is because mixing the two compounds into powder requires heating using a furnace which results in the evaporation process of the compound in liquid form vaporizing into a gas. In addition, there was some mass wasted by distilled water during the washing process.

TABLE 4. Effect of sintering temperature on hydroxyapatite mass efficiency [42]

Temperature (ºC)	Hydroxyapatite mass after sintering (gram)	Hydroxyapatite mass efficiency (%)
700ºC	4.6619	68.55
800ºC	4.5888	67.47
900ºC	3.9036	57.40
1000ºC	3.7734	55.49

As shown in table 4, the increase in sintering temperature causes the efficiency of hydroxyapatite to decrease. Venkatesan and Kim also stated that the efficiency of about 60% indicated that pure hydroxyapatite [28]. The mass efficiency of hydroxyapatite is higher when the sintering temperature is lower. The decrease in the value of hydroxyapatite efficiency in the sintering process is thought to be due to the loss of water content and organic matter contained in the hydroxyapatite powder material of blood clam shells which causes a decrease in hydroxyapatite mass after sintering which similar reported by Riyanto et al. and Al-Sokanee *et al.* [43,44].

CONCLUSION

The main chemical oxide for blood clam shells before calcination is $CaCO_3$ is 99.92% and decreases after calcination in the form of CaO about 99.49%. The high calcium content in blood clam shells makes this material very potential to be used as a raw material for the synthesis of hydroxyapatite. The resulting hydroxyapatite composition contains the main chemical compounds, namely CaO and P_2O_5, with a CaO/P_2O_5 ratio of 1.51 - 1.77. The functional groups show the presence of phosphate (PO_4^{3-}), hydroxyl (OH^-), and carbonate (CO_3^{2-}) indicates hydroxyapatite was formed. The results of the XRD analysis showed that hydroxyapatite has a hexagonal crystal structure. This result is the same as the crystal structure of commercial hydroxyapatite. The purity of the hydroxyapatite produced is not optimum because there is still a secondary phase of HAp decomposition. Hydroxyapatite efficiency value decreased with increasing sintering temperature.

ACKNOWLEDGEMENT

The author would like to thank the University of Hasanuddin, especially the Materials and Energy Laboratory for providing place to complete this research.

REFERENCES

1. F. Arifin, and E. S., Martomi. J. Austenit. **1**, 1-8 (2009).
2. S. H. Saharudina, J. H. Shariffuddina, N. I. A. A. Nordina, and A. Ismaila, Materials Today: Proceedings. **19**, 1208–1215 (2019).
3. A. Indra, R. Firdaus, I. H. Mulyadi, J. Affi, and Gunawarman, Ceram. Int. **46**, 15882-15888 (2020).
4. N. D. Malau, and F. Adinugraha, *In Journal of Physics: Conference Series*. **1563**, 1-8 (2020).
5. Z.Wang, S. Jiang, Y. Zhao, and M. Zeng, Materials Science and Engineering. **105**, 1-7 (2019).
6. M. S. Islam, and M. Todo, Am J Clin. Exp. Med. **3**, 268-274 (2015).
7. L. Anggresani, R. Afrina, A. Hadriyati, Rahmadevi, and M. Sanuddin, J. Katalis. **5**, 54-63 (2020).
8. A. A. Baba, I. T. Oduwole, F. O.Salami, F. A.Adekola, and S. E. Adeboye, African Journals Online. **15**, 435-443. (2013).
9. J. S. Earl, D. J.Wood, and S. J. Milne, *In Journal of Physics: Conference Series*. **26**, 268–271 (2006).
10. I. Kimura, T.Honma, and E. Rima, J. Cer. Soc. Jap. **115**, 888-893. (2007).
11. K. Agrawal, G.Singh, D. Puri, and S. Prakash, J. Miner. Mater. Charact. Eng. **10**,727-734. (2011).
12. S. E. Cahyaningrum, N. Herdyastuty, B. Devina, and D. Supangat, *IOP Conference Series: Materials Science and Engineering*. **299**, 1-5 (2017).
13. J. S. Al-Sanabani, A. A. Madfa, and F. A. Al-Sanabani, Int. J. Biomater, **2013**, 1-12 (2013).
14. B. Musa, I.Raya, and H. Natsir, Int. J. Applied. Chem. **12**, 527-538 (2016).
15. F. Afriani, A. Indriawati, W. B. Kurniawan, Y.Widyaningrum, R. A. Rafsanjani, and Y.Tiandho, Gravity. Jurnal Gravity. **6**, 28-33 (2020).

16. F. W. Puspita, and S. E. Cahyaningrum, UNESA J. Chem. **6**,100-106 (2017).
17. S. Stea, M.Visentin, L.Savarino, M.E. Donati, A. Pizzoferrato, A. Moroni, and V. Caja, J. Mater. Sci. Mater. Med. **6**, 455–459 (1995).
18. G. Muralithran, and S. Ramesh, Ceram. Int. **26**,221-230 (2000).
19. R. F. Siregar, and E. Sulistyowati, Eksergi. **16**, 59-63 (2019).
20. B. D. Cullity, *Elements of X-Ray Diffraction* (Addison-Wesley Publishing Company inc, Notre Dame, 1956).
21. A.J. Awang-Hazmi, A. B. Z. Zuki, M. M.Noordin, A. Jalila, and Y. Norimah, J. Anim. Vet. Adv. **6**, 591-594. (2005).
22. M.Sari, and Y.Yusuf, *In IOP Conf. Series: Materials Science and Engineering*. **432**, 1-9 (2018).
23. K. Dahlan, Int. J. Basic. Applied Sci. **12**,147-151 (2013).
24. R. Ruslan, Thesis, Hasanuddin University, Makassar 2015.
25. P. L. Hariani, M. Said, and Salni, *IOP Conf. Series: Materials Science and Engineer*ing. **509**, 1-9 (2019).
26. D.O. Obadaa, E.T.Daudab, J.K. Abifarina, D. Dodoo-Arhinc, and N. D. Bansode, *Materials Chemistry and Physics*. **239**, 1-9 (2020).
27. K. Prabarakan, and S. Rajeswari, Trends Biomaterials Artificial Organs. **20**, 20-23. (2006).
28. J.Venkatesan, and S. K. Kim, Journal Materials **3**, 4761-4772 (2010).
29. S. Mondal, B. Mondal, A. Dey, and S.S. Mukhopadhyay, J. Mine. Mater. Charact. Eng. **11**, 56-67 (2012).
30. Y. Walendra, Synthesis and Characterization of Porous Hydroxyapatite from Blood Shells with Beeswax Porogen. Essay (IPB. Bogor 2012).
31. J. F.Gomes, C. C. Granadeiro, M. A. Silva, M. Hoyos, R. Silva, and T. Vieira, Int. J. Chem. React. Eng. **6**, 1-15 (2008).
32. K. U., Henggu, B. Ibrahim, and P. Suptijah, Indones. J. Fish. Prod. Process. **22**, 1-13. (2019).
33. Balgies, S.U. Dewi, and K. Dahlan, Proceedings of the National Seminar on Neutron Scattering and X-Rays, Serpong, 2011) 10-13.
34. M. Khoiriyah, and S. E. Cahyaningrum, Unesa J Chem. **7**, 25-29 (2018).
35. A. Singh, Bull Mater Sci. **35**, 1031–1038. (2012).
36. M. Z. A. Khiri, K. A. Matori, N. Zainuddin, C. A. C. Alassan, Z. N. Alassan, N. F. Baharuddin, and M. H. M. Zaid, SpringerPlus. **5**, 1-15 (2013).
37. P.Kamalanathan, S. Ramesh, L.T. Bang, A.Niakan, C. Y. Tan, J. Purbolaksono, H. Chandran, and W. D. Teng, Ceram Int. **40**, 16349–16359 (2014).
38. Hardiyanti, and K. Dahlan, Journal of Biophysics. **8**, 42-48 (2012).
39. M. Z. A. Khiri, K. A.Matori, M. H. M. Zaid, C. A. Che Abdullah, N. Zainuddin, I. M. Alibe, N. A. A. Rahman, and S. A. A. Wahab, Ceramics-Silikáty. **63**,194-203. (2019).
40. Affandi, Amri, and Zultiniar, Jom FTEKNIK. **2**, 1-8 (2015).
41. M. S. Islama, A. M. Z.Rahmanc, M. H. Sharifd, A.Khane, M. A. Al-Mamun, and M.Todo, J. Asian Ceramic Soc. **7**,183–198 (2019).
42. N. Rauf, F. H. Lahu, and S. Suryani, The effect of Sintering Temperature on the Synthesis of Hydroxyapatite From Blood Shells (in Indonesian: Pengaruh Suhu Sintering Terhadap Sintesis Hidroksiapatit Dari Cangkang Kerang Darah) submitted to Physics Nasional Conference October 9, 2021 in Physics Departement University of Hasanuddin (2021), p.75-79.
43. B. Riyanto, A. Maddu, and Nurrahman, JPHPI. **16**,119-132 (2013).
44. Z. N.Al-Sokanee, A. A. H. Toabi, M.J. Al-Assadi, and E. A. Al-Assadi, AAPS pharmacy Science Technology**.** **10**, 772-779 (2009).